Propeller geometry optimization for pressure pulses reduction: an analysis of the influence of the rake distribution

Stefano Gaggero[1], Giorgio Tani[1], Diego Villa[1], Michele Viviani[1], Fabiana Miglianti[1], Pierluigi Ausonio[2], Piero Travi[2], Giovanni Bizzarri[3], Francesco Serra[3]

[1] University of Genoa, Department of Electrical, Electronic, Telecommunications Engineering and Naval Architecture, Via Montallegro, 1, 16145 Genoa.

[2] DETRA Custom Propellers, Genoa, Italy

[3] Azimut|Benetti Group, Varazze, Italy

ABSTRACT

Pressure pulses evaluation is a current issue in high-performance propeller design. Usually, it has been addressed experimentally and numerically but in most cases the analysis has been limited to the verification of a given geometry identified at the end of a traditional design loop. A more direct inclusion of pressure pulses evaluation in the design procedure, for instance by very attractive multi-objective optimization approaches, could be beneficial, especially if higher fidelity codes may be exploited. Among the others, BEM represent an acceptable compromise between computational costs and accuracy, allowing to better considering propeller geometry. However, the direct computation of pressure pulses by means of BEM may be not always reliable, especially in correspondence to heavy cavitation. Hence, further validations are needed, in particular when the influence of geometrical characteristics rarely taken into account, such as rake distribution, are considered. Cavitation tunnel test, BEM and RANS calculations (monitoring cavitation extent and pressure pulses) have been consequently carried out for two propellers, designed for the same functioning conditions with different rake distributions. This allows analyzing capabilities and limitations of these numerical approaches in the light of their possible application in a design by optimization procedure.

Keywords

Propeller pressure pulse, cavitation tunnel tests, Boundary Elements Method, RANS, rake effect.

1 INTRODUCTION

Nowadays the control and reduction of negative effects related to propeller functioning is considered a key point for high quality propeller designs. In this context, propeller cavitation and pressure pulses gained large importance when dealing with applications characterized by high comfort requirements, such as cruise ships and high value pleasure crafts. In parallel to this, the more traditional requirements for speed and efficiency maximization and erosive cavitation avoidance are always present, resulting thus in an increased design complexity.

The traditional design approaches are based on the well-established lifting line and lifting surface methods. In these cases, after the propeller geometry is defined, propeller performances are verified by means of more accurate tools or procedures. These may consist in experimental tests or in computations, adopting more accurate numerical methods like BEM and RANSE. This holds, in particular, for the prediction of pressure pulses and radiated noise, which, usually, cannot be directly included, due to the inherent nature of the traditional design tools, in the design procedure.

The possibility to include these aspects in the design loop, instead, could allow significantly improving the quality of the propeller design, in particular when constraints circa radiated noise and comfort onboard turn into fundamental design goals. A possible solution is the adoption of multi-objective optimization approaches, which allow exploiting codes properly designed for propeller verification. Such codes provide a higher level of accuracy for what regards propeller hydrodynamic performance, starting from the more usual thrust and torque evaluation and including also cavitation and pressure pulses. In these procedures, an unavoidable requirement is the computational efficiency since the optimization procedure may require the definition and the verification of several thousands of different geometries. Consequently, Boundary Elements Methods (BEM) represents usually the most attractive tool for design by optimization activities, being a good compromise between computational time and accuracy of the solution. Their application, as recently demonstrated in literature, was successful in many different cases, including ducted (Gaggero et al., 2012), CLT (Gaggero et al. 2016a, 2016b) and CPP propellers at different pitch conditions (Gaggero et al. 2012, Vestig et al., 2016).

The inclusion in the optimization loop of the evaluation of pressure pulses may result in larger computational times, making also these simplified approaches too onerous. Actually, the unsteady computations needed for the prediction of pressure pulses, even considering fast BEM codes, require significantly more time than the stationary calculations usually adopted in the optimization procedure

with a quasi-steady approach. This suggests the need of simplified criteria to account for these side effects into the design process. In literature, the commonly adopted one considers the pressure pulses reduction as an implicit result of cavitation minimization, de facto avoiding the direct computation of pressure pulses. The shortcoming of such an approach is that it does not take into account pressure pulses induced by the non-cavitating propeller, which, occasionally, may be dominant. In such cases, the simple reduction of cavity area may be ineffective. This because the pressure fluctuations for the non cavitating propeller may vary significantly depending on geometrical characteristics (for instance the rake distribution) or on the radial distribution of load whose effects in the optimization process, consequently, should be considered regardless the risk of cavitation.

In addition, the complete computation of pressure pulses, even if routinely performed in propeller design verification activities, is still challenging, since the reliability of any numerical codes is not fully verified, especially in correspondence to significant cavitation extensions. Actually, when large cavitation extensions are present, potential (and sometime viscous) codes often overestimate the impact of cavitation on the induced pressures, especially for the tone at blade rate. This has been shown for example in Gaggero et al. (2016c) for a fast twin-screw vessel. Similar results have been evidenced by numerical results obtained for the PPTC test case (Kinnas et al., 2015); this important benchmark, moreover, revealed analogous difficulties also when more accurate viscous codes (i.e. LES) are considered. These problems may be as misleading as the simple cavitation minimization criterion, since, by overestimating cavitation contribution on pressure pulse, they practically tend to minimize cavitation giving lower importance to other geometrical factors on pressure pulses amplitude.

In this work, such problems are studied both experimentally and numerically for the case of the propellers of a fast pleasure craft. In order to assess the reliability of the available numerical tools (BEM and RANS) in predicting pressure pulses and in accounting for the influence of less usual geometrical modifications, two alternative design solutions characterized by different rake distributions, namely pointing forward (towards the suction side) and aftward (towards the pressure side), are considered. The considered operational conditions (a relevant shaft inclination and a particularly low functioning cavitation index), typical for this kind of crafts, plus the unsteadiness generated by the shaft angle, represent a very challenging test case to compare the numerical ability of the available codes to tackle the problem of the prediction of the propeller side effects. In the specific, calculations have been carried out using a Boundary Elements Method developed at the University of Genoa (Gaggero et al. 2012) which, as previously mentioned, has been largely adopted for design by optimization of conventional and unconventional propellers, and the StarCCM+ RANS solver (CD-Adapco, 2016). At first, the analyses have been

focused on non-cavitating conditions, by comparing measurements carried out at the cavitation tunnel of the University of Genoa and calculations for the two propellers to analyze the effect of the different rake distributions on pressure pulses and the reliability of numerical calculations in less complicated functioning conditions. Secondly, attention has been focused on cavitation and its effect on pressure pulses. The comprehensive analysis of experiments and simulations provides useful indications for the interpretation of optimization results and for the definition of simplified approaches for the evaluation of pressure pulses to be introduced in such design procedure.

2 CASE STUDY

Both the geometries under investigation are five blade, fixed pitch, propellers designed for a high speed, twin-screw, pleasure craft (Gaggero et al. 2017a, 2017b, Tani et al. 2017). The first propeller (P1501), designed by traditional procedure adopting a lifting line/surface code, is characterized by a rake distribution significantly directed forwards. This particular distribution has been adopted mainly with the aim of increasing propeller efficiency by loading the outer radii sections. This propeller provides already good performance, even if with rather large cavitation extensions at maximum speed, which was generally accepted for the specific application.

As a part of an industrial research project, a second propeller (P1503) was designed by exploiting a multi-objective optimization procedure (Gaggero et al., 2017a, 2017b) with the aim of enhancing propeller cavitating behavior while maintaining, or possibly increasing, the propeller efficiency. As a secondary effect, the reduction in cavitation extension was supposed to enhance propeller performance also in terms of pressure pulses and radiated noise but these quantities were not directly considered during the optimization loop or for the selection of the optimal candidates. From a preliminary analysis, a different rake distribution, directed aftwards, was adopted for this propeller. This was intended to unload the propeller tip and consequently to reduce the cavitation extension; meanwhile the optimization algorithm was forced to compensate the load reduction modifying blade geometry to balance the consequent reduction of efficiency. The new geometry perfectly fulfilled these requirements at design operating conditions at the cost, however, of a relevant cavitation moving to off design conditions. In particular, at higher thrust coefficient with respect to the design point the propeller experienced significant sheet cavitation, even larger than the original one.

These two propellers, whose design procedures and experimental verifications are largely described in Gaggero et al. (2017a), represent a challenging case for the study of pressure pulses and the impact of the design by optimization procedure on these side effects. A first experimental investigation, based on extensive cavitation tunnel test, was presented in Tani et al. (2017). The two propellers were compared in terms of pressure pulses, highlighting the worst performance of the optimized (for cavitation and efficiency) geometry. Supported also by

some simplified computations, the worsening of the pressure pulses behavior in the case of the optimal propeller was mainly ascribed to the effect of the rake distribution.

These aspects are deemed of relevant importance, especially to suitably define an optimization procedure focused on the reduction of propeller pressure pulses. Consequently, it was decided to analyze in details the problem by additional measurements and by including ad-hoc numerical simulations to understand the physical mechanism of the variations of the pressure pulses between the two configurations. This was possible defining a new, and more challenging, experimental setup, with higher shaft inclination, and two load conditions reported in Table 1.

Table 1: Propellers operational conditions.

Operational conditions	K_T	N
Condition 1, no cav.	0.212	5.10
Condition 1 (Design point)	0.212	0.85
Condition 2, no cav.	0.310	6.45
Condition 2 (Off design)	0.310	1.50

In particular, the design point, corresponding to ship maximum speed, is considered, mainly for its practical importance. In addition, also an off-design operational condition, characterized by high thrust coefficient with different cavitation number, has been tested. This latter condition, characterized by relevant sheet cavitation, provides an interesting case study to analyze the influence of this type of cavitation on pressure pulses for propellers in twin-screw configuration and flow unsteadiness mainly driven by tangential components of the velocity field.

3 EXPERIMENTAL SETUP

Cavitation tunnel tests have been carried out at the cavitation tunnel of the University of Genoa. The facility is a Kempf & Remmers closed water circuit tunnel with a squared testing section of 0.57 m x 0.57 m, having a total length of 2 m. The tunnel is equipped with a Kempf & Remmers H39 dynamometer, which measures the propeller thrust, the torque and the rate of revolution. As usual, a mobile stroboscopic system allows visualizing cavitation phenomena on the propeller blades. Moreover, cavitation phenomena visualization in the testing section is also made with three Allied Vision Tech Marlin F145B2 Firewire Cameras, with a resolution of 1392 x 1040 pixels and a frame rate up to 10 fps.

Operational conditions are defined by thrust coefficient and cavitation number. Propeller revolution rate is set to be as higher as possible, respecting the limits of the facility to limit Reynolds effects. Current tests have been carried out mainly at 25 and 22.5 RPS. The presence of possible unwanted resonance phenomena is usually checked during preliminary tests.

The experimental setup is schematically reported in Figure 1. The propeller is tested by placing the dynamometer downstream and adopting a shaft inclination of 11°. The dynamometer is vertically positioned to respect the propeller clearance with the upper observation window of the tunnel test section, reproducing the real clearance (0.23D) between the propeller and the hull. Five differential pressure transducers (KULITE XTL-190M-5G) are considered and arranged as per Figure 2.
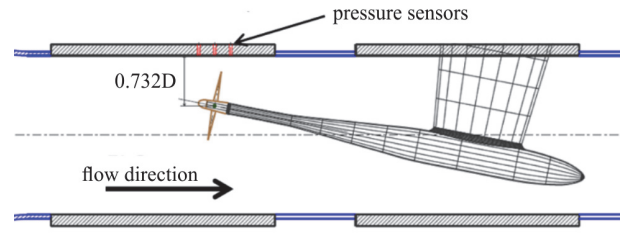

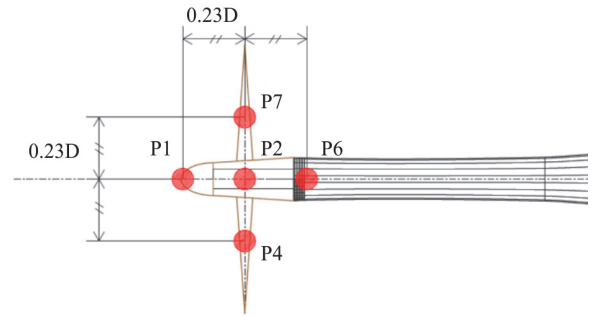Figure 1: Cavitation tunnel configuration: lateral view.

Figure 1: Cavitation tunnel configuration. Sensor position (view from above).

The five sensors signals are acquired simultaneously with the trigger signal, with a sampling frequency of 60 kHz recording 2^{21} samples. From each sensor, the ensemble average of the pressure signal is computed. Amplitude and phase of pressure pulses tonal components are then derived from the harmonic analysis of this ensemble average. Results are then given in non-dimensional form, using the pressure coefficient K_P, defined as:

$$K_P = \frac{p}{\rho N^2 D^2} \qquad (1)$$

where p is the amplitude of the tonal component, N is the propeller rate of revolution, D its diameter and ρ is water density.

4 NUMERICAL METHODS

Two computational codes have been adopted for the present calculations. The first is a Boundary Elements Method developed at the University of Genoa. It is based on the Green second identity to solve the Laplacian equation that is the counterpart of the continuity equation in case of inviscid, irrotational and incompressible flow. The strength of the linearized sources and dipoles placed on the hyperboloidal panels have been obtained satisfying appropriate kinematic and dynamic boundary conditions based on which cavitation, as well as unsteady flow around the propeller, can be addressed (Morino and Kuo, 1974, Fine, 1992, Fine and Kinnas, 1993, Hsin, 1990, Vaz, 2005). The reliability of the unsteady propeller performance, as the cavitation extension, has been previously demonstrated in several papers (Gaggero et al. 2010, Gaggero et al.,

2014). The second is StarCCM+, a commercial viscous flow solver based on the finite volume approach which is able to solve the flow field under the Reynolds approximation which includes the turbulent effects by means of a two equations model (*realizable k-ε*, in present calculations) on a cell centered unstructured mesh (CD-Adapco, 2016). Cavitation is accounted by means of the homogeneous mixture approximation using the *Volume of Fluid* approach to track the liquid/vapor interface. This method, commonly adopted in case of calculations of multiphase incompressible fluids, solely adds a pure convective equation to compute the amount of vapor (or liquid) inside each cell while unmodified momentum equations are solved for the mixture having weighted averaged physical proprieties (density and viscosity) depending on the fraction of each phases. Among the available mass transfer model, the Schnerr-Sauer (Schnerr and Sauer, 2001) approximation was used to evaluate the amount of generated or condensed vapor inside the domain, without taking care of a real compressible approach, de-facto reducing of several orders the computational effort required to compute the acoustic aspects underlying the cavitation phenomena.

Both codes have been adopted to compute the pressure pulses with a setup resembling the experimental facility. With RANS, the test section of the cavitation tunnel, including the dynamometer, has been completely modeled while for BEM calculations a simpler "flat plate" at the right clearance was used to predict pressure pulses. The two numerical setups in terms of both geometry and mesh arrangement are shown respectively in Figures 3 and 4. About 1200 panels per blade have been adopted for BEM calculations to compute both the non-cavitating and cavitating conditions. The flat plate was discretized with 1600 quadrilateral elements. Each simulation requires a computational time of about 15 minutes for the non-cavitating and about one hour when cavitation is included. Calculations run for an equivalent of 8 propeller revolutions (with an equivalent time step of 6 deg.) to avoid the initial numerical transient related to the key-blade approach and to provide a sufficiently long periodic signal to evaluate the blade harmonics. Unsteady viscous RANS calculations were setup with about 7.5 million cells to discretize the entire computational domain, composed by the propeller, the dynamometer and the confined test section of the tunnel. The cells have been further clustered around the blades and close to the positions of the pressure sensors to have a better estimation of the cavitation bubble and limit as much as possible, compatibly with the available computational resources, numerical dissipation. Also in this case, several propeller revolutions are required to achieve a periodic solution after the initial transient. Calculations ran on a medium-end 24 cores workstation for 75 hours each in non-cavitating conditions to complete about 20 propeller revolutions. An equivalent time step of 0.5 deg., together with second order accurate schemes both in space and in time, was used.
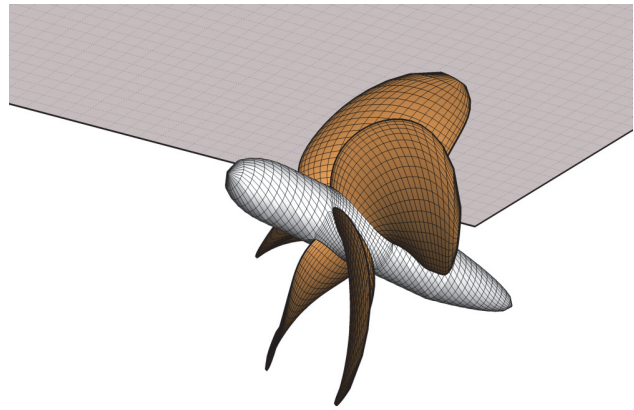

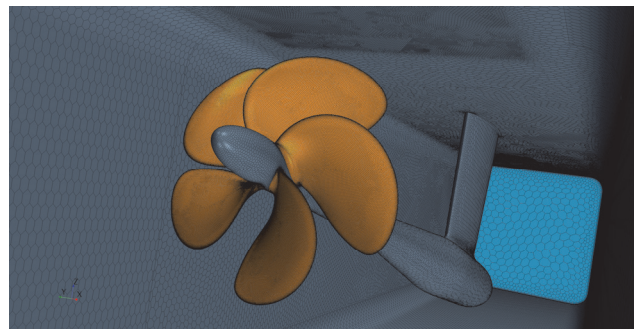Figure 3: Surface mesh for BEM calculations.

Figure 4: Mesh for RANS calculations.

With cavitation turned on, calculation times almost doubled due to the stringent convergence criteria required for multi-phase calculations. In any case, cavitating calculations were initialized with the converged non-cavitating solutions and ran for additional 15 propeller revolutions. Similarly to the experimental post-processing of data, numerical signals were processed extracting their tonal component to be consistently compared with measurements: blade passages were superimposed and averaged to filter out spurious effects related to blade-to-blade different meshes and all the influence of unresolved bubble dynamics, providing smoother signals to be post-processed by means of usual FFT analyses.

5 RESULTS

Results are presented and discussed focusing the attention on the two previously mentioned aspects, i.e. effect of rake distribution and of cavitation extension on pressure pulses. Measurements will be used to analyze the capabilities of the considered numerical methods, identifying their limitations and their sensitivity to local geometrical modifications. These analyses will be reported in terms of tones at blade passage frequency, which usually represent the higher peaks in the pressure pulse spectrum, also by comparing cavitation observations in order to show the relationships between the cavitation extensions and the pressure amplitudes.

5.1 Effect of the Rake Distribution

Propeller pressure pulses are, actually, representative of the flow perturbation due to the passage of the blade and of its pressure field. They are influenced, consequently, by different factors, like the radial load distribution, the load

variations due to non-uniform propeller inflow, the presence of cavitation and, in the end, by the shape of the blade and on how it interacts with the inflow. The blade geometry, in addition, could play a significant role in the "directivity" of the surrounding pressure field, with the rake distribution as the main contributor to this effect.
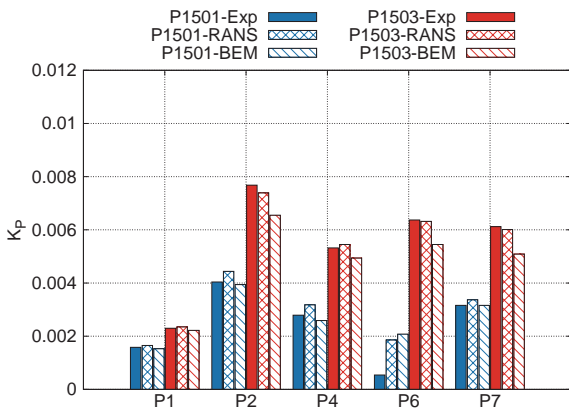

Figure 5: Pressure pulses at blade passage frequency. Condition 1 ($K_T = 0.212$). Cavitation suppression ($\sigma_N = 5.1$).
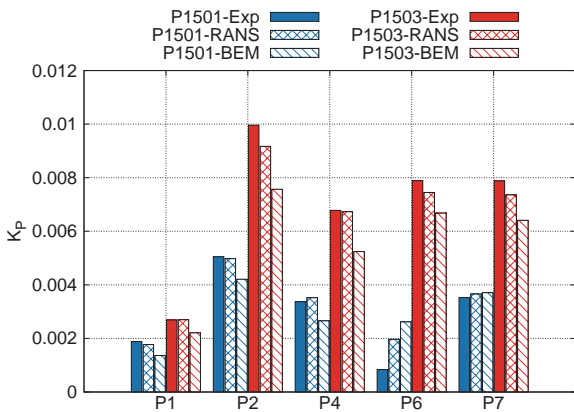

Figure 6: Pressure pulses at blade passage frequency. Condition 2 ($K_T = 0.310$). Cavitation suppression ($\sigma_N = 6.45$).

The influence of the rake distributions has been addressed in the first part of the analysis by considering, for the nature of the phenomena under investigation, only non-cavitating conditions. Non-cavitating pressure fluctuations (measured and computed) at blade rate are reported in Figures 5 and 6 in correspondence to the two thrust coefficients (condition 1 and condition 2) of Table 1.

As it can be seen, the amplitudes of pressure pulses for the two propellers are significantly different for all the sensors. Also the "distribution" of the pressure fluctuation on the flat plate seems different. The propeller with the rake pointing towards the suction side (P1501) generates maximum fluctuation in correspondence to sensor P2, directly above the center of the propeller disk. Amplitudes are similar on starboard and portside and significantly reduced for the downstream sensor (P6)

For the propeller with rake towards the pressure side (P1503) amplitudes are almost doubled, except sensor P1, and rather high, also downstream the propeller plane, while upstream they are more similar to those of propeller P1501. Observed differences are surprisingly high considering that

propellers work at the same functioning conditions and have the same general features. In addition, the highest pressure pulses at blade rate are measured for the propeller whose radial load distribution is more unloaded at tip: this is in contrast to the commonly expected behavior.

The agreement between numerical calculations and experimental measurements is very good, especially in correspondence to the design thrust coefficient. Both the codes, in non-cavitating conditions, are substantially able to predict correctly the pressures behavior in correspondence to the sensors. As a general trend, numerical calculations slightly underestimate pressure pulse amplitudes. BEM results, in particular, underestimate amplitudes also with respect to RANS that, instead, provides more consistent predictions for the loaded condition (condition 2) in correspondence to which BEM shows discrepancies of about 15%. To provide additional information on the effectiveness of the numerical methods, a comprehensive comparison of the pressure pulses up to the fifth harmonic is shown in Figure 7.
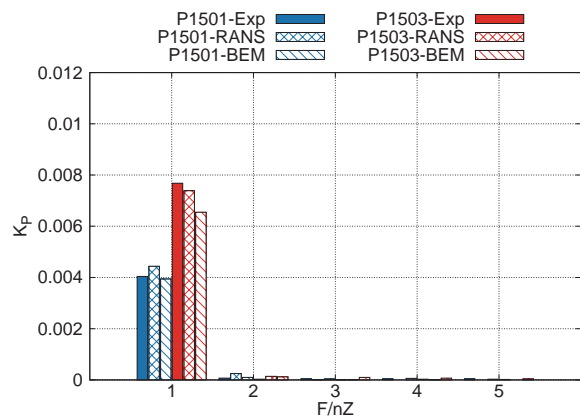

Figure 7: First five harmonics of pressure pulse for sensor P2. Condition 1 ($K_T = 0.212$). Cavitation suppression ($\sigma_N = 5.1$).

Without cavitation, amplitudes at high order harmonics are very low. Both numerical calculations perfectly foresee these features, predicting amplitudes of the same order of magnitude.

This allows exploiting the numerical simulations in order to investigate the reasons leading to the large differences between pressure pulses of the two propellers. To get a deeper insight into the problem, the pressure field around propeller blades is analyzed. RANS computations are considered to this purpose and Figure 8 shows the pressure patterns in the propeller plane for the two propellers. The highest pressure values (in absolute sense) are recorded just below the tip of propeller P1501. This is in good agreement with the tip load increase induced by the rake pointing towards the suction side. However, moving towards the upper part of the domain, which represents the tunnel ceil, the behavior is inverted. Actually, the negative pressure contours for the backward rake propeller P1503 are significantly more directed towards outer radii and in particular towards the tunnel ceil, where pressure sensors are located. This stronger perturbation, moving with propeller rotation, is likely the main responsible of pressure

pulses, hence explaining the differences observed between the two propellers. The radiation towards the outward direction is reduced by the shape of the blade with forward rake, despite the higher values on blades surface, in accordance with results of Kappel propellers, which present an even more evident rake distribution pointing at tip to the suction side (Andersen et al., 2005).
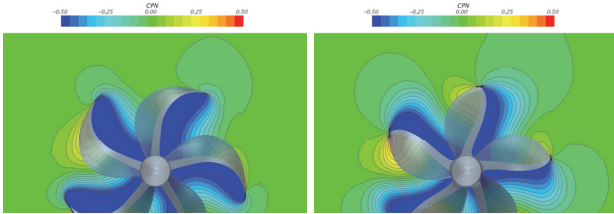

Figure 8: Pressure field around propeller, propeller P1501 on the left, propeller P1503 on the right.

A similar analysis has been previously proposed in Tani et al. (2017). In that case, the comparison was carried out computing the pressure distributions around the propellers in steady conditions. Results showed a very good correlation between the amplitude of pressure pulse at blade passage frequency and the circular pressure distribution around the propeller. Present computations, modelling more accurately the propeller functioning in non-stationary conditions, provide more reliable and complete information on pressure pulses, thus allowing to confirm the outcomes of the previous study. Pressure distributions in non-stationary conditions are different, as obvious because of the varying load, but they maintain same features observed in steady conditions. This means that distributions may be estimated also with simpler (steady) calculations. These simplified results may be not sufficiently accurate to estimate the absolute pressure pulses but they may allow ranking different blade geometries in terms of induced pressure accounting, even if in an approximate way, for specific influences of geometrical characteristics usually not considered for efficiency- or cavitation free- based designs. Such computations may represent a suitable tool for the estimation of non-cavitating pressure pulses in the framework of an optimization procedure, especially considering that for similar computations, the efficient BEM instead of the proposed RANS could be successfully employed.

5.2 Effect of Cavitation Extension

The second part of the analyses is focused on the discussion of the effect of cavitation on pressure pulses. At first, the attention is devoted to the analysis of the cavitation extensions. This provides useful data to investigate the correlation existing between measured pressure pulse and cavitation patterns, both in terms of cavitation typology and extensions. In addition, it allows to validate the capabilities of the computational tools to predict cavitation, which is the starting point for the reliable computation of pressure pulses in cavitating functioning. Condition 1 (maximum speed) is considered at first. Experimental cavitation observations are summarized in Figure 9. As it can be seen, both propeller experience tip vortex and bubble cavitation. The latter, occurs on the whole suction side of the blade at 90°. As far as the extension of cavitation on blades is concerned, the two propellers are quite similar.
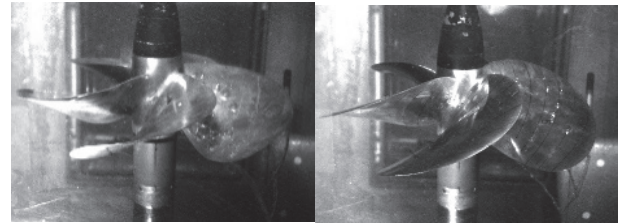

Figure 9: Experimental cavitation observations for condition 1: P1501 on the left, P1503 on the right.

The occurrence of bubble cavitation, however, is significantly more frequent and intense for propeller P1501 (Gaggero et al. 2017a, 2017b, Tani et al. 2017). Actually, even if at the maximum speed condition bubble cavitation is present in both cases, its inception is significantly delayed in the case of the optimized propeller P1503. This was indeed one of the main objectives of the optimization procedure. The complete behaviors of the inception for both the propellers are reported in (Gaggero et al. 2017a, 2017b, Tani et al. 2017).

In agreement with their intrinsic limitations, both BEM and RANS simulations, whose results are shown in Figure 10 and 11, partially succeed in predicting the area where cavitation may occur but are (obviously) not able to model the random behavior of single bubble cavity. Actually, due to the adopted cavitation model and mesh arrangements, it is only possible to evaluate the type of occurred cavitation by analyzing sections pressure distributions: minima are placed around mid-chord, thus suggesting the presence of bubble cavitation instead of sheet cavitation. The adoption of the homogeneous mixture approach simply neglects the bubbly nature of the phenomenon and a single region of vapour, instead than multiple, interacting bubbles, is predicted starting, in accordance with any semi-empirical mass transfer models, from the regions where the pressure falls below the vapour tension. Analogously for BEM, the development of mid-chord (bubble) cavitation is addressed exactly with the same model developed for leading edge phenomena, using the Villat-Brillouin criteria (Mueller and Kinnas, 1999) only to identify reasonable cavity detachment points.
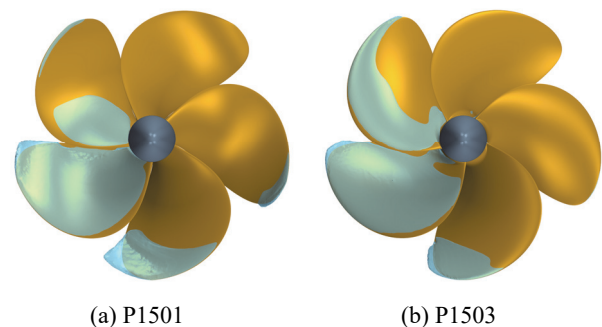

(a) P1501   (b) P1503

Figure 10: RANS predicted cavitation extension for condition 1.
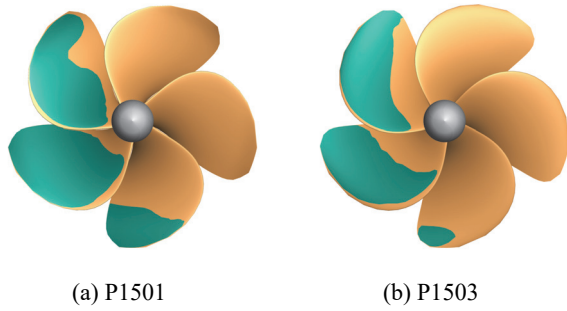
(a) P1501   (b) P1503

Figure 11: BEM predicted cavitation extension for condition 1.

In addition, computed cavitation extensions do not rank correctly the two propellers. Cavitation seems larger (close to 90 deg. position) with the optimized propeller, contrarily to experimental results and the outcomes of the design activity (Gaggero et al., 2017a). Exactly to account for these limitations of the cavitation models, the design was mainly carried out on the basis of simpler criteria on non-cavitating pressure distributions and reasonable assumptions circa the nature of cavitation depending on the occurrence and the positions, along the chord, of the minimums of the pressure: those of the original propeller features lower negative pressure; hence anticipated and more developed cavitation. A detailed description of the design criteria and of the results of the optimization activities can be found in Gaggero et al., (2017a).
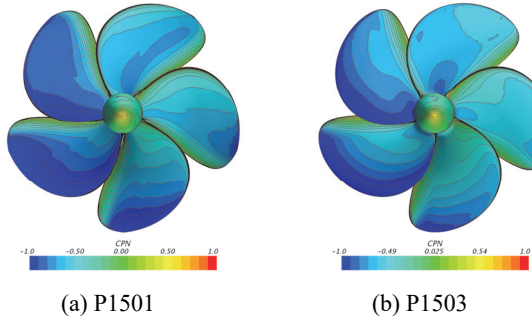

(a) P1501   (b) P1503

Figure 12: RANS predicted non-cavitating pressure coefficient distributions ($C_{PN} = 2(p - p_{ref.})/(\rho N^2 D^2)$) for condition 1.

Figure 12, for the sake of completeness, compares the pressure coefficient distributions computed by RANS on the propeller blades for functioning condition 1. Zones where the pressure falls below the design cavitation index of 0.85, identified by the dark blue contour, are sensibly more extended along the propeller revolution and sensibly affect mid-chord in the case of the reference geometry P1501. The approximate cavitation model smear, by means of an excessively overestimated region of vapor, the differences visible by non-cavitating calculations.

When the off-design condition is considered, the cavitation pattern is completely different, as shown by the observations reported in Figure 13. In this case, large suction side sheet cavitation and tip vortex cavitation occur for both propellers. As previously mentioned, the sheet cavity is more extended in the case of the optimized propeller (P1503). Sheet cavitation, extending from 0.8R to the tip, is present starting slightly after the 12 o'clock
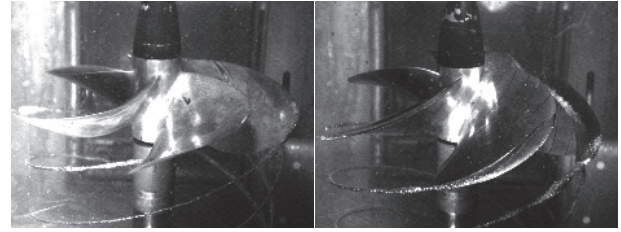

Figure 13: Experimental cavitation observations for condition 2: P1501 on the left, P1503 on the right.
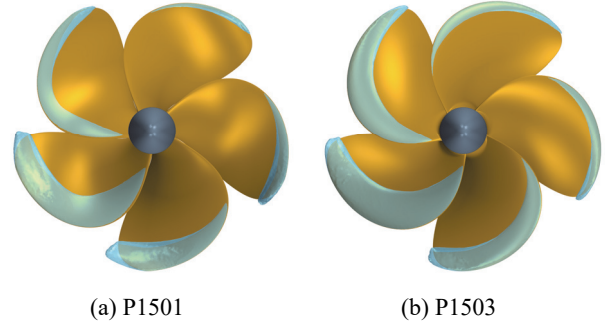

(a) P1501   (b) P1503

Figure 14: RANS predicted cavitation extension for condition 2.
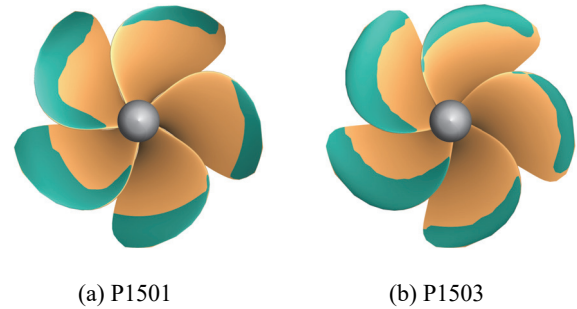

(a) P1501   (b) P1503

Figure 15: BEM predicted cavitation extension for condition 2.

position, while at 90° on starboard a larger cavity is observed from 0.5R. On the contrary, for the original propeller (P1501), sheet cavitation is not present around the 12 o'clock position, but it quickly assumes significant extensions on the blade at 90° on starboard, starting from about 0.7R.

Generally, these cavitation patterns are predicted with reasonable accuracy by the numerical simulations, as shown in Figures 14 ad 15. However, both methods tend to slightly overestimate the extension of the sheet cavity, which at 90° angular position reaches the blade root. This discrepancy with respect to experiments may be related also to the development of the boundary layer in model scale tests. Laminar flow regions may be present at inner radii while viscous calculations are forced to pure turbulent conditions and no transition model has been presently taken into account.

The first step for the analysis of the effects of cavitation on pressure pulses is represented by the comparison of the experimental measurements with and without cavitation, reported in Figures 16 to 19. As a general comment, the effects of cavitation observed during experiments seem rather limited. Some exceptions are present: for the original propeller, condition 1, tones measured by sensors P4, P6

and P7 show appreciable variations. For sensor P4 the pressure fluctuation with cavitation is reduced, while for sensor P6 it is increased from a very low value. As a matter of fact, the most remarkable increase of pressure pulse amplitude is observed for sensor P7. This behavior may be related to the large bubble cavitation at 90°.
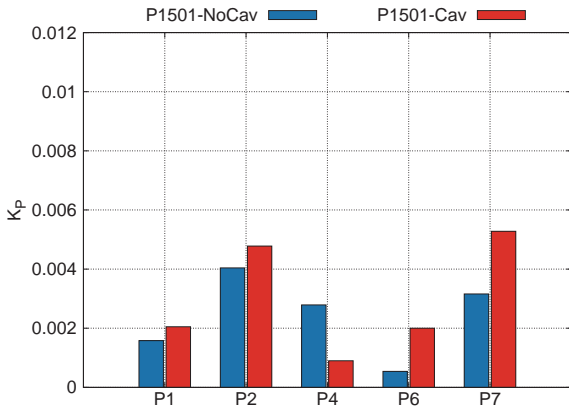

Figure 16: Pressure pulse tone at blade rate. Propeller P1501, Condition 1, with ($\sigma_N = 0.85$) and without ($\sigma_N = 5.1$) cavitation.
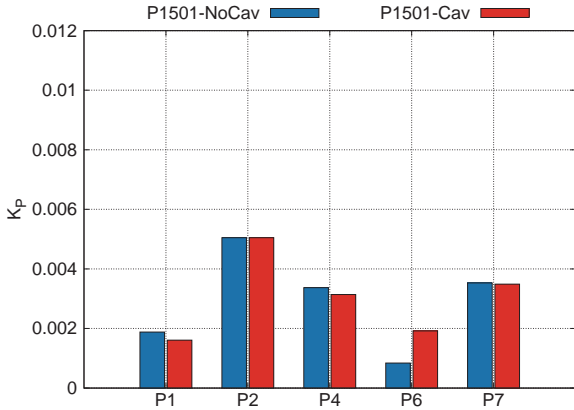

Figure 17: Pressure pulse tone at blade rate. Propeller P1501, Condition 2, with ($\sigma_N = 1.5$) and without ($\sigma_N = 6.45$) cavitation.

Actually, this phenomenon is stronger for the propeller with larger bubble cavitation and it is observed for the starboard sensor, just above the blade at 90°. As already mentioned, bubble cavitation is expected to produce high broadband pressure fluctuations instead of a significant tone at blade rate, thus this result could appear quite surprising. However, it has to be remarked that in general bubble cavitation may produce high levels of pressure fluctuation and noise. The occurrence of bubble cavitation around the 90° position, combined with the varying distance from the sensors, may result in a periodic modulation of its random nature, thus increasing also the tone at blade rate. A similar behavior is observed for the optimized propeller at maximum speed condition, even if in this case the difference with respect to the non-cavitating condition is smaller. In addition, for both propellers, the increase of the tone for sensor P7 at starboard seems to occur simultaneously to the reduction of the tone on portside (Sensor P4).
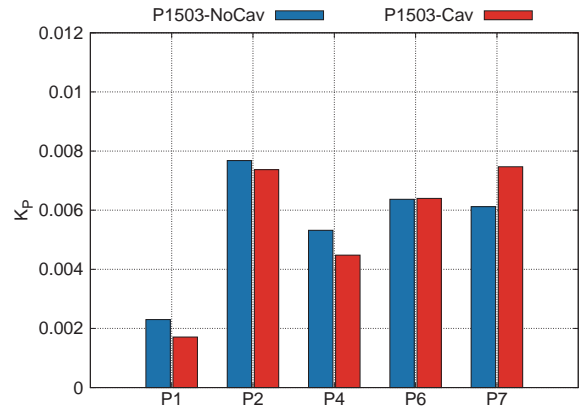

Figure 18: Pressure pulse tone at blade rate. Propeller P1503, Condition 1, with ($\sigma_N = 0.85$) and without ($\sigma_N = 5.1$) cavitation.
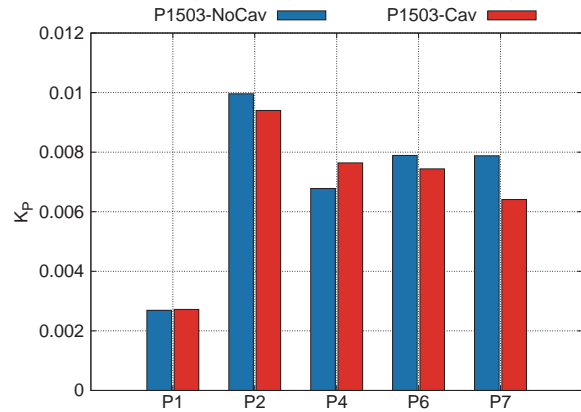

Figure 19: Pressure pulse tone at blade rate. Propeller P1503, Condition 2, with ($\sigma_N = 1.5$) and without ($\sigma_N = 6.45$) cavitation.

The interpretation of such correlation, which however should be verified considering further measurements, is not straightforward and perfectly exemplifies the complexity of the phenomenon. It is interesting to point out that, usually, higher amplitudes at blade rate are expected in the case of large sheet cavitation, due to the large periodic volume pulsation of the sheet cavity. However, this is not confirmed by current experiments. Actually, moving to the off-design condition, only measurements from sensor P6 show some differences for the original propeller, while for the optimized propeller the effect of cavitation seems negligible.

Summarizing, experiments show limited effects of present cavitation patterns on pressure pulse at blade rate. This result is quite remarkable, especially if compared with the observed effects of the rake distribution. Of course, it has to be observed that this does not hold for higher order harmonics or broadband fluctuations, which on the contrary are significantly increased by cavitation (Tani et al. 2017). However, the extensive study of such fluctuation components would need further analyses, which are beyond the aims of present work.

The results of numerical calculations are compared to measurements in Figures 20 and 21.
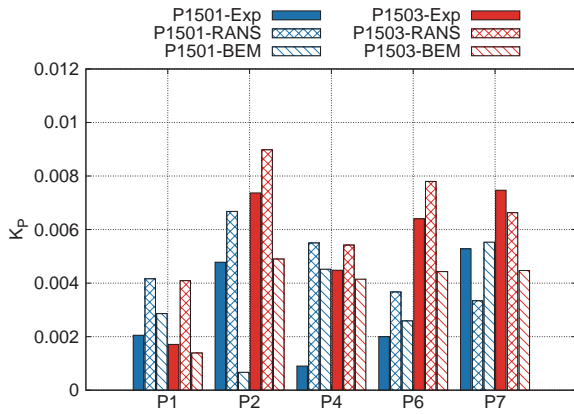
Figure 20: Pressure pulses at blade passage frequency. Condition 1 ($K_T = 0.212$), with cavitation ($\sigma_N = 0.85$).
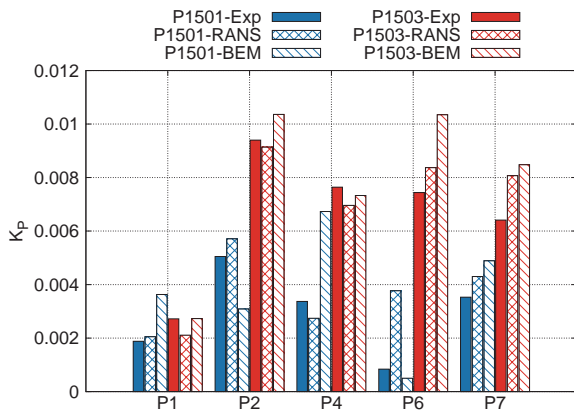

Figure 21: Pressure pulses at blade passage frequency. Condition 2 ($K_T = 0.310$), with cavitation ($\sigma_N = 1.5$).

In general, the agreement is worse, but still reasonable, than that observed in non-cavitating conditions. As far as RANS computations are concerned, small discrepancies with experiments are observed, with the general tendency to overestimate pressure pulses for condition 1 (Figure 20). This, in principle, agrees with observed difficulties of the method to correctly model the bubble cavitation in condition 1, which directly reflect on pressure pulse computation. Calculations are able to predict only the presence of a large cavity, extended up to the trailing edge of the blades, whose dimensions vary smoothly during propeller revolution. Pressure pulses are computed accordingly: such dynamic behavior results in a periodic volume variation, which is expected to impact significantly on the tone at blade rate. On the contrary, real cavitation is significantly less extended and characterized by a random nature.

For functioning condition 2, results of the RANS model (Figure 21) are significantly improved, with a fair agreement with experiments that confirms the good reliability of this model when mainly sheet cavitation is present. As a summary, both RANS and experiments show that cavitation in condition 2, despite the significant extension, does not affect remarkably pressure pulse at blade rate. On the contrary, RANS slightly overestimates cavitation effects (again very reduced) for condition 1, due to the presence of bubble cavitation. As far as experiments

are concerned, the blade rate harmonic is slightly increased by cavitation in functioning condition 1 only above the position where large bubble cavitation occurs at each blade passage (P7). On the contrary, RANS calculations overall overestimate pressure pulses regardless the location of the pressure probes due to the very large sheet cavity instead of bubble cavitation, even if P7 pressure increase is not captured (actually, P7 pressure is nearly kept constant).

In case of cavitating BEM calculations, differently from what observed in non-cavitating conditions, the analysis is more complex, as already evidenced by many authors (Kinnas et al., 2015). The agreement with experiments, even if not very poor on average, varies significantly depending on sensor, propeller and functioning conditions, and it is difficult to identify a unique trend. The uncertainties due to cavitating panels at bubble trailing edge could produce local fluctuations of the perturbation potentials that become disturbances for the induced pressure pulses. The prediction of the sheet cavity extension, indeed, is an iterative and discrete (i.e. the cavity closure is achieved on the last panel of each circumferential cavitating strips having a positive cavity thickness). Together with the key-blade approach, in which the influence of each blades further from the key one is accounted by using the solution history of the key-blade itself, this discrete approach could induce, blade passage per blade passage, revolution per revolution, differences also well after the initial transient. These differences could result in few more (or less) cavitating panels with different potentials whose influence on the periodicity of induced pressure pulses could be significant, especially when larger (and beyond the applicability of the thin sheet cavity assumption) bubbles are predicted, sometimes nullifying the role of sensitivity analyses.

Similarly to the non-cavitating conditions, a final analysis of the pressure pulse harmonics (up to the 5th order, in this case) for a selection of points (in this case sensor P2) could be worth to further investigate the reliability of numerical calculations. Results, summarized in Figures 22 and 23, confirm the acceptable reliability of the RANS computations. According to experiments, also pressure pulses at multiples of the blade rate, up to the 5th harmonics, are only weakly influenced by cavitation. An increase of the second harmonic is observed for condition 2 with both propellers (larger in the case of P1503). This trend is qualitatively captured by RANS calculations, even if discrepancies exist. As an example, RANS fails to predict the above-mentioned increase of the second harmonic for condition 2 while it shows an opposite behaviour in condition 1, consequently overestimating the second harmonic. Nevertheless, the order of magnitude of higher order harmonics is comparable with those of experiments, and, accordingly, always significantly lower than that of the tone at blade rate. BEM, as for (and even more than) the first harmonic, predicts very high and not consistent amplitudes at multiples of blade rate, confirming that pressure pulses computations with this method are more problematic and less accurate.
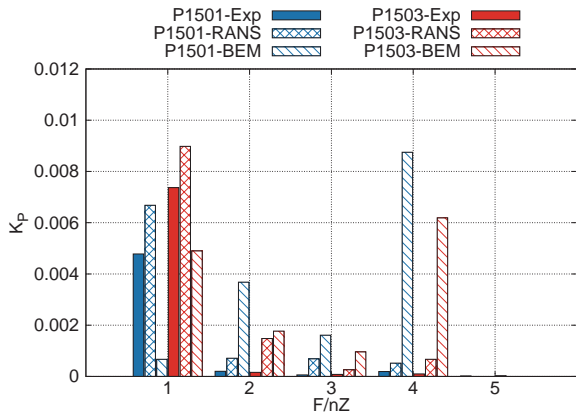
Figure 22: First five harmonics of pressure pulse for sensor P2. Condition 1 (K_T = 0.212) with cavitation (σ_N = 0.85).
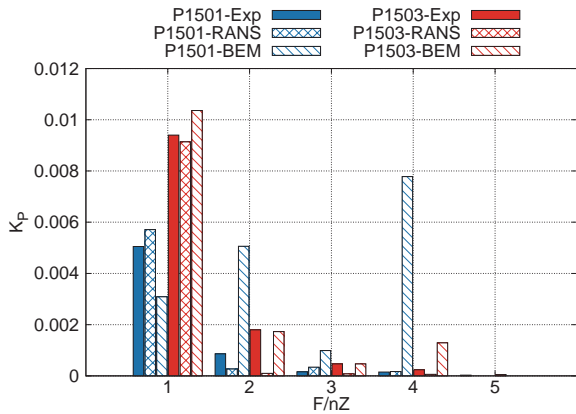

Figure 23: First five harmonics of pressure pulse for sensor P2. Condition 2 (K_T = 0.310) with cavitation (σ_N = 1.5).

6 Conclusions

In the present work, the problem of propeller pressure pulses prediction has been addressed, analyzing two propellers designed with considerably different rake distributions, for the same application. For the two propellers, model tests at cavitation tunnel with inclined shaft have been carried out, considering two different propeller loadings (design point plus a more heavily loaded off-design condition). In both cases, tests have been carried out with cavitation suppression and in actual cavitating conditions, characterized mainly by bubble cavitation (design condition) and leading edge sheet cavitation (heavily loaded condition), plus a strong tip vortex, observed in both cases. Numerical calculations using BEM and RANS have been simultaneously carried out exactly in the same functioning conditions.

The analysis of the large amount of data collected during measurements allows tackling many different aspects related to propeller pressure pulses: the effect of the rake distribution, the influence of cavitation (with two different typologies) and, finally, the reliability of numerical calculations in dealing with these phenomena in both non-cavitating and cavitating conditions.

A remarkable difference between the two propellers in terms of pressure pulses, related to the influence of the rake distribution, has been evidenced. The amplitudes of pressure pulses produced by the backward rake propeller are on average twice the values measured for the forward rake geometry. This effect has been observed both in non-cavitating and in cavitating conditions.

Results of numerical simulations, in correspondence to the non-cavitating conditions, were in very good agreement with experiments, confirming the effectiveness of these tools in predicting propeller pressure pulses without cavitation. In addition, the analysis of simulation results allowed to gain a better insight into the effect of the rake distribution, showing its strong influence on the pressure field induced by the propellers and in particular on its directivity.

This different directivity of blade pressure field explains the lower pressure pulse at blade rate for the forward propeller despite the higher tip loading and larger cavitation of this propeller.

In cavitating conditions the experimental campaign demonstrated that, even considering the unsteady functioning given by the remarkable shaft inclination, all the phenomena (bubble cavitation, sheet cavitation, tip vortex) have a very limited impact on propeller induced pressure fluctuations at blade rate (first harmonic). This finding cannot be considered as a general rule, however it is confirmed by other cases reported in literature (Kinnas et al. 2015, Li et al. 2015, Johansson et al. 2015, Firenze and Valdenazzi, 2015), especially with similar configurations, typical of twin screw vessels or pleasure crafts.

From a numerical point of view, the analysis allowed to confirm the existence of non-negligible drawbacks in the application of BEM approaches, which tend in general to overestimate the effect of cavitation. In the present case, this has been observed mainly by the results in correspondence to the higher order harmonics, but similar discrepancies were already evidenced also for the first harmonic. It appears that BEM codes are not very robust when cavitating conditions are considered and the focus is on pressure pulses; results are considerably affected by the calculation setup, and small changes may results in large variations of pressure pulses. On the contrary, the predicted cavity extensions are in a reasonable agreement with the experimental observations (in correspondence to the heavily loaded condition) and with RANS calculations, always within the inherent limitations of the applied cavitating models.

RANS, in the end, appears definitely more robust, allowing to have a fair prediction (only slightly overestimated, in these simulations) of pressure pulses. This overestimation is observed mainly when bubble cavitation, that is the weakness of multiphase mixture approaches, is addressed. In this sense, these results confirm once more that the simplified *VoF* approach, not being able to track the real cavitation dynamics, significantly affects the prediction of cavitation extension and, in turn, the resultant pressure pulses.

Anyhow, the collected results are of great interest in view of the application of these codes in a design by

optimization activity. In particular, it is clear that it could be beneficial to separately consider different components of pressure pulse. In many cases, the reduction of tone at blade rate may be achieved simply reducing it in non-cavitating conditions; from this point of view, both BEM and RANS calculations appear well suited for a correct ranking of different geometries, also considering non-usual variations of rake distribution. Possible simplified strategies in order to evaluate the effects of geometrical changes with a reduced computational effort (e.g. with stationary calculation), as already presented in Tani et al. (2017) are worth being investigated in future. In parallel, the reduction of the broadband component of the pressure pulses, which is important as well for a high-performance propeller design, could instead be monitored by the usual criteria on minimization of the steady cavity extension, as routinely and successfully applied in the context of a design by optimization still based on BEM calculations, without the burden and the unreliability of unsteady cavitating calculations.

REFERENCES

Andersen, P., Friesch, J., Kappel, J.J., Lundegaard, L. and Patience, G. (2005). ' Development of a Marine Propeller with Nonplanar Lifting Surfaces', Marine Technology, **43**-3, pp. 144 – 158.

Bertetta, D., Brizzolara, S., Gaggero, S., Savio, S. & Viviani, M. (2012). 'CPP propeller cavitation and noise optimization at different pitches with panel code and validation by cavitation tunnel measurements', Ocean Engineering, **53**, pp. 177-195.

CD-Adapco (2016). 'Star-CCM+ 11.06.011 Users Guide'.

Fine, N.E. (1992). 'Nonlinear Analysis of Cavitating Propellers in Nonuniform Flow', PhD Thesis, Massachusetts Institute of Technology.

Fine, N. E. & Kinnas, S. A. (1993). 'A Boundary-Element Method for the Analysis of the Flow around 3-D Cavitating Hydrofoils', Journal of Ship Research, **37**(3), pp. 213 – 224.

Firenze, E., & Valdenazzi, F. (2015). 'A method to predict underwater noise from cavitating propellers', Proceedings of OCEANS 2015, IEEE, Genoa, Italy.

Gaggero, S., Villa, D. & Brizzolara, S. (2010). 'RANS and panel methods for unsteady flow propeller analysis', Journal of Hydrodynamics, **22**(5B-1), pp. 547 – 552.

Gaggero S., Rizzo C.M., Tani G. and Viviani M. (2012). 'EFD and CFD design and analysis of a propeller in decelerating duct', International Journal of Rotating Machinery.

Gaggero S., Villa D. & Viviani M. (2014). 'An investigation on the discrepancies between RANSE and BEM approaches for the prediction of marine propeller unsteady performances in strongly non-homogeneous wakes', ASME 2014 33rd International Conference on Ocean, Offshore and Artic Engineering, OMAE 2014, San Francisco, USA.

Gaggero, S., Gonzalez-Adalid, J. & Perez Sobrino, M. (2016a). 'Design of Contracted and tip loaded propellers by using boundary element methods and optimization algorithms', Applied Ocean Research, **55**, pp. 102 – 129.

Gaggero, S., Gonzalez-Adalid, J. & Perez Sobrino, M. (2016b). 'Design and Analysis of a new generation of CLT propellers', Applied Ocean Research, **59**, pp. 424-450.

Gaggero, S., Tani, G., Villa, D., Viviani, M., Conti, F., & Vaccaro, C. (2016c). 'Assessment of different methods for the prediction of marine propellers induced pressures', In Maritime Technology and Engineering III: Proceedings of the 3rd International Conference on Maritime Technology and Engineering (MARTECH 2016), Lisbon, Portugal.

Gaggero, S., Tani, G., Villa, D., Viviani, M., Ausonio, P., Travi, P., Bizzarri, G. & Serra, F. (2017a). 'Efficient and multi-objective cavitating propeller optimization: an application to a high-speed craft', Applied Ocean Research, **64**, pp. 31-57.

Gaggero, S., Tani, G., Villa, D., Viviani, M., Ausonio, P., Travi, P., Bizzarri, G. & Serra, F. (2017b). 'Application of multi-objective optimization based design to high-speed craft propellers', Proceedings of the fifth International Symposium on Marine Propulsors, smp'17, Espoo, Finland.

Hsin, C.Y. (1990). 'Development and analysis of Panel Methods for Propellers in Unsteady Flows', PhD thesis, Massachusetts Institute of Technology.

Johansson, A. T., Hallander, J., Karlsson, R., Långström, A., & Turesson, M. (2015), 'Full scale measurement of underwater radiated noise from a coastal tanker' Proceedings of OCEANS 2015, IEEE, Genoa, Italy.

Kinnas, S.A., Abdel-Maksoud, M., Barkmann, U., Lubke, L. and Tian, Y. (2015). 'Proceedings of the Second Workshop on Cavitation and Propeller Performance', Proceedings of the Fourth International Symposium on Marine Propulsors, smp'15, Austin, Texas, USA.

Li, D. Q., Hallander, J., Johansson, T., & Karlsson, R. (2015). 'Cavitation dynamics and underwater radiated noise signature of a ship with cavitating propeller', Proceedings of the VI International Conference on Computational Methods in Marine Engineering, MARINE2015, Rome Italy.

Morino, L. & Kuo, C.C. (1974). 'Subsonic Potential Aerodynamic for complex configuration: a general theory', AIAA Journal, **12**, pp. 191 – 197.

Mueller, A.C. & Kinnas, S.A. (1999). 'Propeller sheet cavitation predictions using a panel method', Journal of Fluids Engineering, **121**, pp. 282 – 288.

Schnerr G. & Sauer J. (2001). 'Physical and numerical modeling of unsteady cavitation dynamics', Proceedings of the 4th International Conference on Multiphase Flow, New Orleans, Luisiana, USA.

Tani, G., Villa, D., Gaggero, S., Viviani, M., Ausonio, P., Travi, P., Bizzarri, G. & Serra, F. (2017). 'Experimental investigation of pressure pulses and radiated noise from two alternative designs of the propeller of a high-speed craft', Ocean Engineering, **132**, pp. 45 – 69.

Vaz, G. (2005). 'Modelling of Sheet Cavitation on Hydrofoils and Marine Propellers using Boundary Element Methods', PhD Thesis, Technical University of Lisbon – IST.

Vesting, F., Gustafsson, R., & Bensow, R. E. (2016). 'Development and application of optimisation algorithms for propeller design', Ship Technology Research, **63**(1).